

# Theoretical Studies on the Structure and Aromaticity of $\text{Ti}_2\text{P}_6^+$

Wei-Qi Li,<sup>†</sup> Wei Quan Tian,<sup>\*,‡</sup> Ji-Kang Feng,<sup>\*,†,§</sup> Zi-Zhong Liu,<sup>†,⊥</sup> Ai-Min Ren,<sup>†</sup> and Gang Zhang<sup>†</sup>

State Key Laboratory of Theoretical and Computational Chemistry, Institute of Theoretical Chemistry, Jilin University, Changchun 130023, China, Department of Material Sciences, Faculty of Engineering Sciences, Kyushu University, 6-1 Kasugakoen, Kasuga, Fukuoka, 816-8580, Japan, College of Chemistry, Jilin University, Changchun 130023, China, and Chemistry & Environment Science College, Inner Mongolia Normal University, Huhehaote 010022, China

Received: March 8, 2005; In Final Form: July 26, 2005

Cationic cluster  $\text{Ti}_2\text{P}_6^+$  has been studied within density functional theory. The structure of this cluster is predicted to be a slightly distorted tetragonal prism. The dissociation energy of this cationic cluster is higher than that of the known sandwich compound,  $[(\text{P}_5)_2\text{Ti}]^{2-}$ , because of the different bonding in these two compounds. In  $\text{Ti}_2\text{P}_6^+$ , the hybridization of P atoms of the ring is  $\text{sp}^3$ . The bonding between the metal atoms and the P ring is mainly  $\sigma-\pi$ . While in  $[(\text{P}_5)_2\text{Ti}]^{2-}$ , the P atoms take  $\text{sp}^2$  hybridization, the bonding between the metal atom and the rings is the typical  $\pi-\pi$  interaction. The electronic delocalization is another stabilizing factor for  $\text{Ti}_2\text{P}_6^+$ . The nuclear independent chemical shift indicates that  $\text{Ti}_2\text{P}_6^+$  is a three-dimensional aromatic molecule. The predicted infrared and NMR help to identify the  $\text{Ti}_2\text{P}_6^+$  conformations in experiment.

## 1. Introduction

Almost all transition metals can form phosphorus compounds.<sup>1–6</sup> There are more than 200 transition bimetallic phosphorus clusters. These transition bimetallic phosphorus clusters can form many linear, cyclo, and caged structures. However, the chemical bonds in the metallic phosphorus compounds are difficult to determine because of the versatile bonding between the transition metals and phosphorus atoms. The lack of experimental information on the structure and bonding nature of these metallic phosphorus clusters necessitates the theoretical studies on these clusters.<sup>6</sup>

P/Ti clusters were investigated before computationally.<sup>7–9</sup> Liu et al. reported the mass spectra for titanium phosphorus clusters by laser vaporization of phosphorus and Ti powders. During the laser induced photodissociation of the phosphorus titanium clusters, they discovered two dissociation paths for  $\text{Ti}_2\text{P}_6^+$ .<sup>10,11</sup> Recently Urneúzýius et al. synthesized a new sandwich compound of phosphorus with titanium and did detailed structural and bonding analysis on the compound.<sup>12</sup> This work attracted extensive attention from both experimentalists and theoreticians. The focus of this work is on the theoretical studies of  $\text{Ti}_2\text{P}_6^+$ .

In a previous report,<sup>9</sup> the standard hexagonal bipyramid was predicted to be the most stable conformation for  $\text{Ti}_2\text{P}_6^+$ . Our present studies find that this conformation is not the most stable conformation. Accurate calculations indicate that the most stable structure for  $\text{Ti}_2\text{P}_6^+$  is a slightly distorted tetragonal prism. As in fact, the similarly distorted phosphorus compound<sup>13</sup>  $[(\text{Cp}^*\text{Ti})_2(\mu-\eta^3:\eta^3-\text{P}_6)]$  was discovered in experiment in which the two Ti atoms have a  $\text{C}_5\text{H}_5^-$  ligand on each Ti atom. With the aid of the molecular orbital energy diagram, Chandrasekhar<sup>17</sup> explained in detail the cause of phosphorus ring distortion and pointed out that charge delocalization stabilizes the molecule a good

deal. However, the author did not make a detailed investigation of the charge delocalization effect on the stability of the molecule, which is the important part of our work.

Aromaticity<sup>15–21</sup> is an important concept in organic chemistry, it explains the structural stability and chemical reactivity of molecules. The common character of these molecules with aromaticity is that these molecules are planar with delocalized  $\pi$  orbitals. Recent studies extended the concept of aromaticity to organometallic<sup>22–25</sup> and all-metal<sup>26–30</sup> systems. It is believed that the concept of aromaticity connects with three-dimensional structure.<sup>31–33</sup> It was found that not only  $\pi$  bond but also  $\sigma$  bond has electron delocalization. For the sake of quantitative analysis, some criteria such as structural (geometric), energetic, magnetic, and reactivity related ones were proposed for the aromaticity study. Which one is the best criterion for aromaticity is still in debate.<sup>34–37</sup> Among the widely used magnetic criteria for aromaticity and antiaromaticity, the nuclear independent chemical shift (NICS)<sup>38–40</sup> is a simple while efficient probe for this purpose. The validation is corroborated through its wide application in ring compounds, atomic clusters, molecular transition state, and transition metal compounds. The calculations of NICS at four points in  $\text{Ti}_2\text{P}_6^+$  confirm that this cluster is a three-dimensional aromatic molecule.

## 2. Calculation Method

Density functional theory based hybrid method B3LYP<sup>41</sup> in combination with Gaussian basis set, 6-311+G(2df),<sup>42–45</sup> has been employed in searching for the most stable structure for the  $\text{Ti}_2\text{P}_6^+$  cluster starting from a wide variety of structures. The second-order derivatives of total energy with respect to nuclear coordinates (Hessian) were calculated to verify the nature of the stationary point on the potential energy surface through vibrational frequency calculations. The stationary point is a minimum if there is no imaginary frequency (eigenvalue for Hessian). It is a saddle point if there is at least one imaginary frequency. The relative energies of the conformations were

<sup>†</sup> Institute of Theoretical Chemistry, Jilin University.

<sup>‡</sup> Kyushu University.

<sup>§</sup> College of Chemistry, Jilin University.

<sup>⊥</sup> Inner Mongolia Normal University.

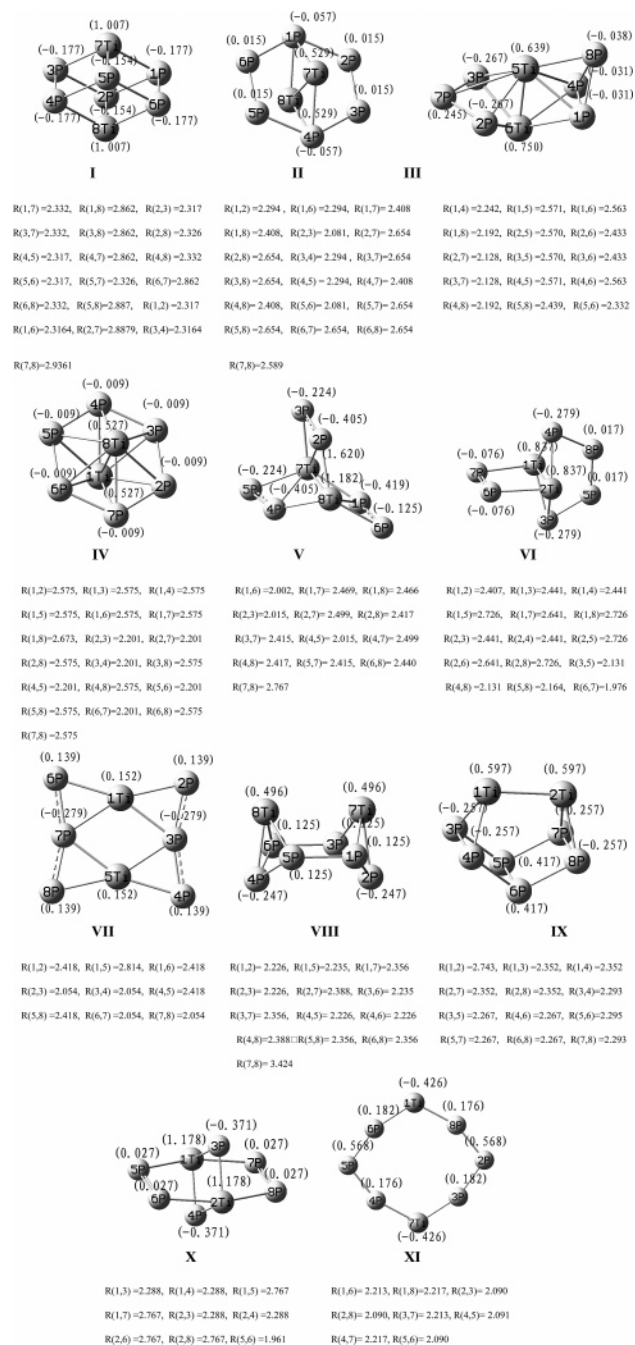


**Figure 1.** The atomic charges and the main bond lengths (Å) of  $\text{Ti}_2\text{P}_6^+$  cluster isomers.

further calculated with the Møller–Plesset perturbation theory method up to second-order perturbation (MP2)<sup>46</sup> with the 6-311+G(2df) basis set based on the B3LYP/6-311+G(2df) geometries. Natural bond orbital (NBO)<sup>47–49</sup> analysis and NICS calculations were performed for conformations I and IV at the B3LYP/6-311+G(2df) level of theory. All the calculations were carried out with the Gaussian 03 quantum chemical package<sup>50</sup> and the molecular orbitals were plotted with the Molden program.<sup>51</sup>

### 3. Results and Discussions

**A. Molecular Structure and Electronic Properties.** The optimized stable structures with low energy at the B3LYP/6-311+G(2df) level of theory for  $\text{Ti}_2\text{P}_6^+$  are shown in Figure 1. The relative stability and nature of the stationary points are

summarized in Table 1. At this level of theory, the most stable conformation is a slightly distorted tetragonal prism with  $C_{2h}$  symmetry. The second most stable conformation with  $D_{2h}$  is just 5.58 kcal/mol above conformation I. To confirm the DFT prediction, the relative energies of the conformations were calculated with MP2, QCISD, and CCSD(T) (because of the large consumption of QCISD and CCSD(T) methods, we only calculate the energies of conformation I and conformation II with these two methods since the energy of conformation III is well above that of conformation I) with the DFT optimized geometry. At all three levels of theory, conformation I is still the most stable conformation. The relative energy sequence of the MP2 level agrees well with the B3LYP predictions. At the QCISD and CCSD(T) levels, the energy of conformation I is 5.52 and 10.80 kcal/mol lower than that of conformation II, respectively. The highest occupied molecular orbital and the lowest unoccupied molecular orbital gap (HOMO–LUMO gap) is 1.578 eV for conformation I. The first vertical ionization energy (10.643 eV) for conformation I is 1.531 eV larger than the HOMO energy (−9.112 eV). At the B3LYP/6-311+G(2df) level of theory, the calculated energy difference between the  $^2A_g$  electronic state and the  $^4A_g$  electronic state for conformation I is 1.708 eV, while the energy difference between the  $^2A_g$  electronic and the  $^6A_g$  electronic state is 3.830 eV, i.e., the  $^4A_g$  electronic state is 2.122 eV more stable than the  $^6A_g$  electronic state. All these energetic predictions indicate that the doublet is the ground state of conformation I.

With the same method and basis set, the structures (as shown in Figure 2) of  $[(\text{P}_5)_2\text{Ti}]^{2-}$  and the  $\text{P}_5$  ring were optimized to compare the calculated structure with available experimental data to validate the method employed (B3LYP/6-311+G(2df)) for the prediction of  $\text{Ti}_2\text{P}_6^+$ . This also provides reference for the predicted dissociation energy. The predicted P–P bond distance in  $[(\text{P}_5)_2\text{Ti}]^{2-}$  is 2.17 Å and the experimental value is 2.16 Å. The calculated Ti–P bond distance is 2.59 Å and the measured one is 2.56 Å. The predicted distance from the Ti atom to the center of the phosphorus ring is 1.797 Å and it is the same as the experimental one.<sup>10</sup> For the  $\text{P}_5$  ring, the calculated P–P bond distance is 2.12 Å and the measured one is in the range from 2.08 to 2.12 Å. The comparison of the predicted bond distances with the measured ones justifies the application of B3LYP/6-311+G(2df) in the structural prediction for Ti/P clusters.

The structures of conformations I, II, and IV in Figure 1 are very similar. In these conformations, the hexagonal phosphorus ring bonds to the two Ti atoms from two sides. The phosphorus ring in conformation IV is a planar canonical hexagon. The hexagon in conformation II is also planar but slightly distorted. The phosphorus rings in conformation I have a chair shape. Vibrational frequency calculations identify that three conformations are minima. The electronic state of conformation IV is  $^4A_1$ . There is no stable structure with  $D_{6h}$  symmetry in the  $^2A_1$  electronic state. There are four long P–P bonds in conformation II and they are easily broken, thus conformation II is unstable with respect to the P–P bond distances.

Conformations III and V are also minima on PES with low symmetry ( $C_s$ ). The phosphorus atom P7 in conformation III has large positive charge. The energy of conformation III is 12.49 or 25.48 kcal/mol higher than that of conformation I at the B3LYP/6-311+G(2df) or MP2/6-311+G(2df) level of theory, respectively, whereas the two Ti atoms in conformation V have large positive charges thus resulting in strong electrostatic repulsion between them. The energy of conformation V is 22.97 or 57.86 kcal/mol higher than that of conformation I

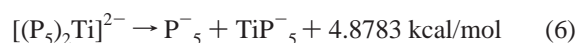
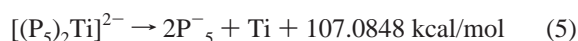
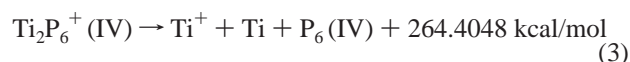
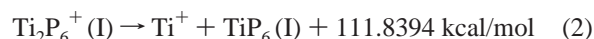
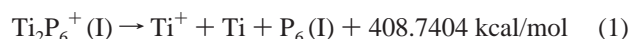
**TABLE 1: Total Energy (au), Number of Imaginary Frequency, and Relative Energy (kcal/mol) of Isomers of the  $\text{Ti}_2\text{P}_6^+$  Cluster**

isomer	symmetry	NIF <sup>a</sup>	total energy (relative energy)			
			B3LYP/ 6-311+G(2df)	MP2/ 6-311+G(2df)	QCISD/ 6-311+G(2df)	CCSD(T)/ 6-311+G(d)
I	$C_{2h}$	0	-3747.1025(0.00)	-3742.3093(0.00)	-3742.3112(0.00)	-3742.1358(0.00)
II	$D_{2h}$	0	-3747.0936(5.58)	-3742.3073(1.26)	-3742.3024(5.52)	-3742.1186(10.80)
III	$C_s$	0	-3747.0826(12.49)	-3742.2687(25.48)		
IV	$D_{6h}$	0	-3747.0770(16.00)	-3742.2643(28.24)		
V	$C_s$	0	-3747.0659(22.97)	-3742.2171(57.86)		
VI	$C_{2v}$	2	-3747.0418(38.09)	-3742.2357(46.18)		
VII	$D_{2h}$	1	-3747.0142(55.41)	-3742.2370(45.37)		
VIII	$C_{2v}$	2	-3747.0017(63.25)	-3742.1067(127.13)		
IX	$C_{2v}$	2	-3746.9344(105.48)	-3742.2171(57.86)		
X	$D_{2h}$	5	-3746.9162(116.91)	-3742.0802(143.76)		
XI	$C_{2h}$	2	-3746.8892(133.85)	-3741.9393(232.18)		

<sup>a</sup> NIF: number of imaginary frequencies.

at the B3LYP/6-311+G(2df) or MP2/6-311+G(2df) level of theory, respectively. The rest of the conformations have at least one imaginary frequency, thus they are transition state or high order saddle point on PES. In conformations VI and X, there are  $\text{P}_2$  groups with weak interaction with Ti and these  $\text{P}_2$  groups can detach from the conformation with a small amount of energy according to the bond distances. Conformations VII and XI are planar while the transition metal prefers three-dimensional structures, thus these two conformations have high energy. Conformation VIII comprises two roofs connected through two P–P bonds. However, these two P–P bonds are weak with long bond distances (2.235 Å) thus rendering conformation VIII unstable. For conformation IX, the vibrational frequency calculations indicate that it is a second-order saddle point. Its energy is 105.48 kcal/mol higher than that of conformation I at the B3LYP/6-311+G(2df) level of theory.

In the most stable conformation, conformation I, the average Ti–P bond distance (2.33 Å) is shorter than the Ti–P single bond<sup>53</sup> (2.42 Å). The shrink of the Ti–P bond distances indicates strong interactions between Ti and P in conformation I. To verify this observation, we design a series of reactions to calculate the dissociation energy of the homolytic and the heterolytic bond cleavage to compare the stability of conformations I, IV, and  $[(\text{P}_5)_2\text{Ti}]^{2-}$ :



The phosphorus rings in the above equations,  $\text{P}_6(\text{I})$  ( $C_{2h}$ ) and  $\text{P}_6(\text{IV})$  ( $D_{6h}$ ), and the products  $\text{TiP}_6(\text{I})$  ( $C_s$ ),  $\text{TiP}_6(\text{IV})$  ( $C_{6v}$ ), and  $\text{TiP}_5(C_{5v})$  are optimized based on the corresponding partial structures in the reactants at the B3LYP/6-311+G(2df) level of theory as shown in Figure 2.  $\text{P}_6(\text{I})$  ( $C_{2h}$ ) and  $\text{P}_6(\text{IV})$  ( $D_{6h}$ ) are not the most stable structure.  $\text{P}_5^-$  is the most stable conformation and  $\text{TiP}_5$  is a local minimum on PES.  $\text{TiP}_6(\text{I})$  is a local minimum and  $\text{TiP}_6(\text{IV})$  is the most stable conformation.

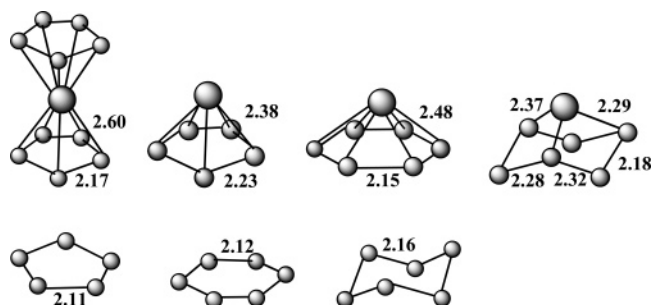


**Figure 2.** The optimized structure of  $[(\text{P}_5)_2\text{Ti}]^{2-}$  (with  $D_{5h}$  symmetry) and the optimized structures of  $\text{TiP}_5$  (with  $C_{5v}$  symmetry),  $\text{TiP}_6$  (with  $C_{6v}$  and  $C_s$  symmetry),  $\text{P}_5^-$  (with  $D_{5h}$  symmetry), and  $\text{P}_6$  (with  $D_{6h}$  and  $C_{2h}$  symmetry) at the B3LYP/6-311+G(2df) level of theory.

The calculations find the order of relative stabilities based on the homolytic dissociation energies to be conformation I > conformation IV >  $[(\text{P}_5)_2\text{Ti}]^{2-}$  and the order of relative stabilities based on the heterolytic dissociation energies to be conformation I > conformation IV >  $[(\text{P}_5)_2\text{Ti}]^{2-}$ .

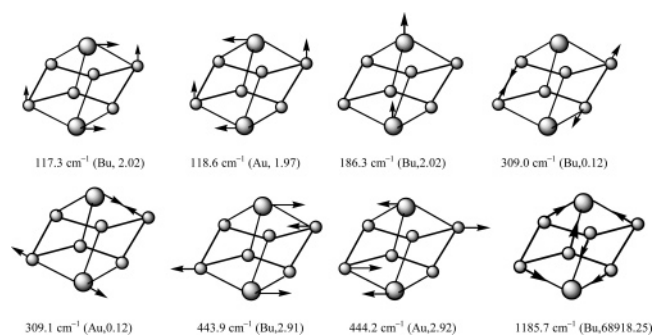
The origin of the order for the relative stability is explored in terms of the structure of these clusters. Among these conformations, the hybridization of P is different in different conformations. All the P atoms in conformation IV are within a plane with  $\text{sp}^2$  hybridization. The interaction between P and Ti in this conformation is  $\pi$ - $\pi$  type, whereas the six P atoms in conformation I form a chair structure similar to the chair cyclohexane. The average  $\angle\text{PPP}$  angle is  $104.0^\circ$ . The optimized typical  $\text{sp}^3$  hybridized  $\angle\text{HPH}$  angle in  $\text{PH}_3$  is  $93.5^\circ$ . If the effects of the lone pair electrons in  $\text{PH}_3$  and of the two Ti atoms in conformation I are taken into account, the rationale on the  $\text{sp}^3$  hybridization in conformations I is justified. The  $\sigma$  and  $\pi$  bonding characters between P and Ti atoms in conformation I is clearly manifested in its molecular orbitals in Figure 4. Such bonding in conformation I results in shorter bond distances and higher homolytic dissociation energy than their counterpart bond distances and homolytic dissociation energy in conformation IV.

According to the heterolytic dissociation energy, the energies released in reactions 2 and 4 are much higher than those in reaction 6. The high heterolytic dissociation energy for conformation I is mainly because of its different bonding from that in conformations IV and  $[(\text{P}_5)_2\text{Ti}]^{2-}$ . In conformation IV, besides the interaction between Ti and P atoms, the two Ti atoms have strong bonding, while the Ti–Ti interaction in conformation I is weaker because of its longer Ti–Ti bond distance than that in conformation IV. The bonding in these two conformations



**TABLE 2: Electron Configurations of  $\text{Ti}_2\text{P}_6^+$  Conformation I**

atom	no.	natural electron configuration
P	1	[core]3s(1.71)3p(3.25)3d(0.05)4p(0.01)
P	2	[core]3s(1.71)3p(3.26)3d(0.05)4p(0.01)
P	3	[core]3s(1.71)3p(3.25)3d(0.05)4p(0.01)
P	4	[core]3s(1.71)3p(3.25)3d(0.05)4p(0.01)
P	5	[core]3s(1.71)3p(3.25)3d(0.05)4p(0.01)
P	6	[core]3s(1.71)3p(3.26)3d(0.05)4p(0.01)
Ti	7	[core]4s(0.34)3d(2.93)4p(0.03)4d(0.12)
Ti	8	[core]4s(0.34)3d(2.93)4p(0.03)4d(0.12)

**CHART 1: The Major Infrared Active Vibrational Mode of the  $\text{Ti}_2\text{P}_6^+$  Conformation I<sup>a</sup>**

<sup>a</sup> The number in parenthesis is intensity in KM/mol.

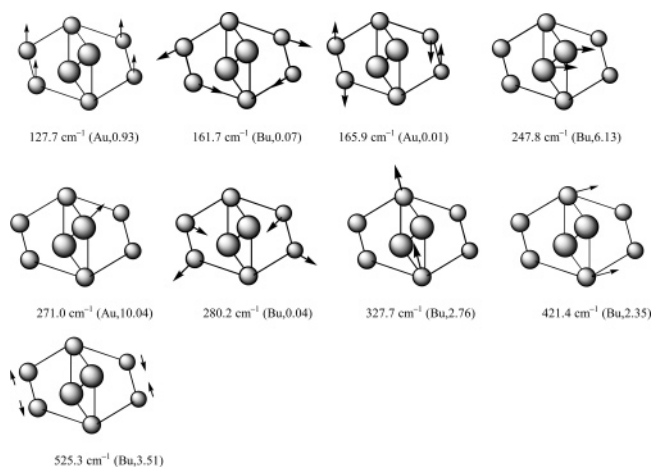
is corroborated from the NBO analysis (the Ti–Ti bond order in conformations IV and I is 0.2651 and 0.2448, respectively). Such large difference in heterolytic dissociation energy indicates the important role of the Ti–Ti bond to molecular stability. However, the overall bonding in conformation I makes this conformation the most stable conformation.

The NBO analysis (in Table 2) indicates that charge transfer in Ti occurs from 4s to 3d and 4d atomic orbitals, while the direction of charge transfer in P is from 3s to 3p. Because of the important roles of d and p orbitals in bonding, such charge transfers facilitate the covalent bonding between Ti and P. One can see that the two Ti atoms have positive charge and all P atoms have negative charges. It is believed that the high negative charge on P and low oxidation valence state expedites the formation of  $\pi$  bonds between the P ring and the transition metals.

**B. IR and NMR Spectra for Conformations I and II.** To assist the identification of the  $\text{Ti}_2\text{P}_6^+$  cluster, the IR and NMR spectra of conformations I and II are calculated at the B3LYP/6-311+G(2df) level of theory.

The most characteristic vibrational modes of two conformations, along with the normal coordinate vectors (arrows), are shown in Charts 1 and 2, respectively. For conformation I, the vibrational mode at 117.34  $\text{cm}^{-1}$  is a rocking of the molecule with respect to the P2TiP5Ti8 plane. The vibrational mode at 118.58  $\text{cm}^{-1}$  is a rocking in the direction perpendicular to the P2TiP5Ti8 plane. The vibrational mode at 186.25  $\text{cm}^{-1}$  is attributed to the Ti–Ti unit back–forward motion along the TiTi direction. The most intense vibrational mode is at 1185.67  $\text{cm}^{-1}$  with much stronger intensity than the rest of the vibration modes. It is Ti–P bond stretching as shown in Chart 1. This infrared active vibrational mode serves as the characteristic IR mode for conformation I.

In the IR spectra of conformation II, on the other hand, there is no IR peak above 1000  $\text{cm}^{-1}$ . There are two strong absorption peaks at 247.8 and 271.0  $\text{cm}^{-1}$ , respectively. The major IR active modes are shown in Chart 2. The most intensive peak is back–forward arching of the molecule along the TiTi direction and it

**CHART 2: The Major Infrared Active Vibrational Modes of the  $\text{Ti}_2\text{P}_6^+$  Conformation II<sup>a</sup>**

<sup>a</sup> The number in parenthesis is intensity in KM/mol.

can serve as the characteristic peak for the IR of conformation II. The IR spectra of conformations I and II facilitate distinguishing these two conformations in experiment.

NMR chemical shifts are an important property of a molecule and are useful tools to identify the molecular structure. For conformation I, two  $^{31}\text{P}$  NMR signals are predicted to have chemical shifts of  $\delta = -277.02$  (P2 and P5 atoms) and  $-275.76$  ppm (P1, P3, P4, and P6 atoms), respectively. Obviously, the strong deshielding of  $^{31}\text{P}$  NMR chemical shifts is due to the delocalization of electrons in conformation I. In the NMR spectra of conformation II, three sets of  $^{31}\text{P}$  NMR signals are predicted with chemical shifts of  $\delta = -679.28$  (P1 and P4 atoms), 105.433 (P2 and P5 atoms), and 171.83 ppm (P3 and P6 atoms), respectively. It indicates that P2, P3, P5, and P6 are shielded while P1 and P4 are deshielded. This is caused by the stronger interactions between P2 and P4 atoms with Ti atoms than those between P2, P3, P5, and P6 with Ti atoms.

**C. Aromaticity.** As to the molecular structure, all the same kinds of bond lengths are equal in conformation IV with  $D_{6h}$  symmetry (P–P bond 2.201 Å, Ti–P bond 2.575 Å). For conformation I, the longest Ti–P bond (2.3325 Å) is 0.0059 Å longer than the shortest Ti–P bond (2.3266 Å). The difference between the longest P–P bond (2.3179 Å) and the shortest P–P bond (2.3164 Å) is only 0.0015 Å. Within the prediction precision, the Ti–P and P–P bonds have equal bond distances, respectively. We believe that the similar average of bond length in these two conformations results from electron delocalization. In addition, in conformations I and IV, both HOMOs are nonbonding molecular orbitals. There are five  $\pi$  molecular orbitals (HOMO-2, HOMO-5, HOMO-6, HOMO-7, and HOMO-8) and two multiple center molecular orbitals (HOMO-10 and HOMO-16) in conformation IV as shown in Figure 3. HOMO-1 is a  $\sigma$  bond between Ti atoms. Similarly, conformation I has five  $\pi$  molecular orbitals (HOMO-1, HOMO-6, HOMO-7, HOMO-8, and HOMO-10) and two multiple center molecular orbitals (HOMO-12 and HOMO-16) as shown in Figure 4. In general the existence of metal–ring  $\pi$  bonds or multiple center bonds ensures the existence of three-dimensional aromaticity. In particular, this is the case for a ring compound of a heavy element with diffusive electronic structure such as P.

NICS is an efficient and simple magnetic criteria for aromaticity. Negative NICS indicates aromaticity and positive NICS indicates antiaromaticity. A very small NICS value means nonaromaticity. The NICSs at some points in conformations I

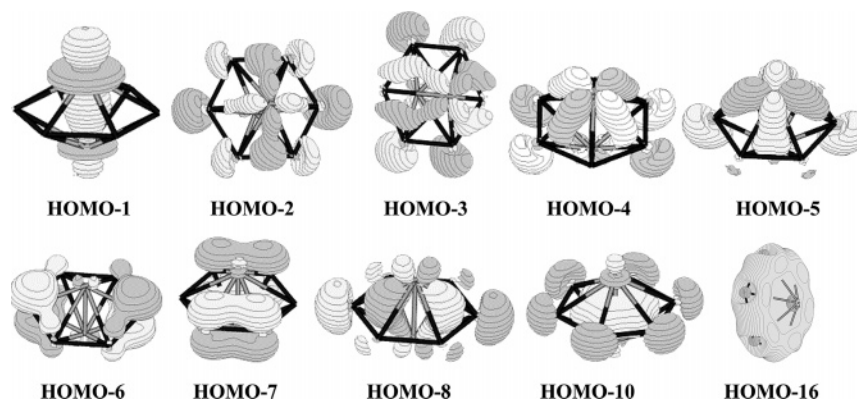


**Figure 3.** The frontier occupied molecular orbitals of  $\text{Ti}_2\text{P}_6^+$  conformation IV.

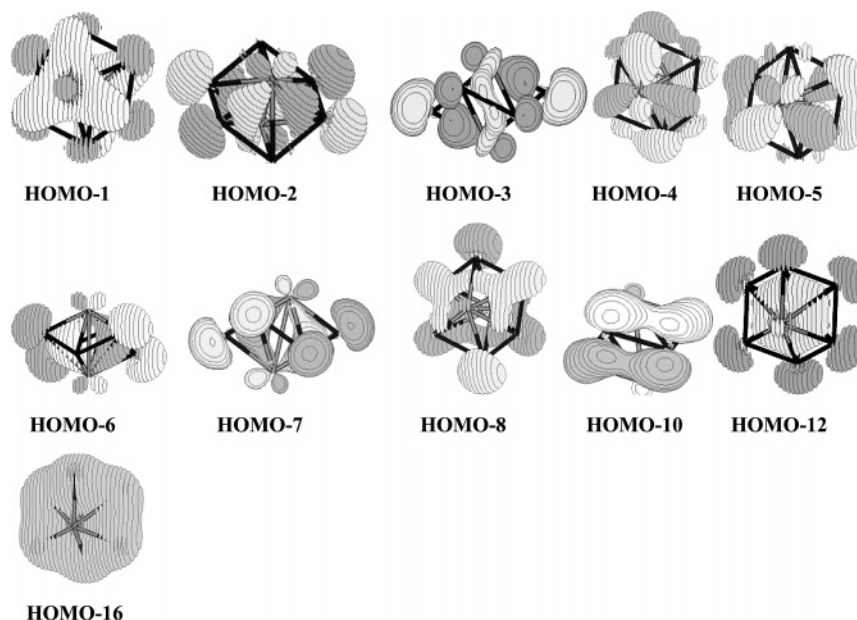


**Figure 4.** The frontier occupied molecular orbitals of  $\text{Ti}_2\text{P}_6^+$  conformation I.

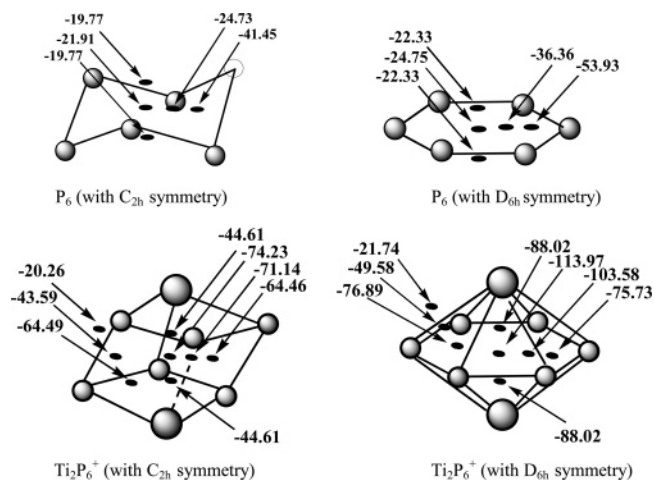


**Figure 5.** NICS values at all points in planar  $\text{P}_6$ , distorted  $\text{P}_6$ , and  $\text{Ti}_2\text{P}_6^+$  conformations I and IV.

and IV and the corresponding planar  $\text{P}_6$  ring and  $\text{P}_6$  chair structure are shown in Figure 5.

The ring centers, the points 0.5 Å below and 1.0 Å above the ring centers, have large negative NICS indicating the aromaticity of the two conformations. The decomposition of NICS indicates that the NICS( $\pi$ ) has higher diamagnetism in the planar ring. However, in the planar ring, the paramagnet-

ism of NICS( $\sigma$ ) partially cancels the contribution of NICS( $\pi$ ) diamagnetism. On the contrary, both the NICS( $\pi$ ) and NICS( $\sigma$ ) are diamagnetic in the chair structure, thus resulting in larger NICS(tot) than that in the planar structure. It is noteworthy that, although the chair structure does not have the typical  $\pi$  orbitals in benzene, there is a similar delocalized  $\pi$  orbital in the chair structure as shown in Figure 6 because of the delocalized outer shell structure of P atoms.

In conformations I and IV, the calculated NICS for all points are negative and these values are more negative than that of the corresponding points in the isolated P rings, which indicates the more delocalized electronic structure after formation of P ring metal clusters. The NICSs of the three points along the Ti–Ti axis in conformation IV are more negative than their counterpart points in conformation I. This is due to the closer Ti–Ti bond distance in conformation IV and the diffusive electronic structure of Ti atoms—the three points have strong effects from the covalent interactions of the Ti atoms. Taking these effects into account, the NICSs for the points 0.5 Å above and 1.0 Å below the equator plane of conformations I and IV are calculated as shown in Figure 5. The NICS values of such points decrease (particularly in conformation IV) with distance from the equator plane with respect to the points along the Ti–Ti axis. The NICS at the center of side planes of these two conformations are also calculated to check the electron delocalization. The NICSs of these points are close in the two

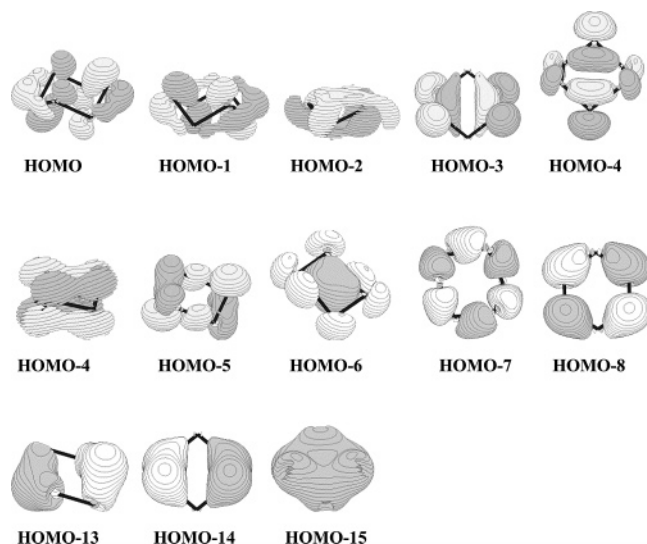


**Figure 6.** The frontier occupied molecular orbitals of the most stable conformation of  $P_6$  cluster with chair structure.

conformations. In both conformations, the NICS value at the inner side of the plane is much larger than that at the outer side.

According to the calculations, one can see that conformations I and IV are obviously aromatic molecules. This is one of the major factors for the stability of the hexagonal bipyramid structure. However, one should note that aromaticity is just one important factor while not the decisive factor in the stability of a structure.

#### 4. Conclusions

Within density functional theory with the 6-311+G(2df) basis set, the electronic structure and stability of the  $Ti_2P_6^+$  cluster is investigated. The most stable conformation of this cluster is a slightly distorted tetragonal prism. According to the dissociation energy calculations, the dissociation energy of conformation I is much larger than that of conformation VI and the typical sandwich  $[(P_5)_2Ti]^{2-}$  cluster. This reveals that Ti has a stronger interaction with the phosphorus ring in conformation I. The predicted IR and NMR spectra of conformations I and II facilitate to identify these two conformations in experiment. The molecular orbital analysis manifests that the interaction between Ti and P ring includes both  $\pi-\pi$  and  $\sigma$  bonds, thus with high bonding energy. The large negative NICS values indicate that this molecule is a three-dimensional aromatic compound and corroborate the previous proposal.<sup>16</sup> The isoelectronic clusters  $Ti_2N_6^+$ ,  $Ti_2As_6^+$ , and  $Ti_2(CH)_6^+$  may also exist because of possible aromaticity; such clusters await future investigation.

**Acknowledgment.** This work is supported by the National Nature Science Foundation of China (20473031) and the Key Laboratory for Supramolecular Structure and Material of Jilin University. W.Q.T. thanks the Japan Society for the Promotion of Science for financial support and Prof. Yuriko Aoki for her hospitality.

#### References and Notes

- (1) Franzen, H. F. *Structure & Bonding in Metal-Rich Pnictides, Chalcides & Halides. Prog. Solid State Chem.* **1978**, *12*, 1.
- (2) Rundqvist, S. *Binary Transition Metal Phosphides. Arkiv. Kemi.* **1962**, *20*, 67.
- (3) Schnering, Von, H. G.; Honle, W. *Phosphides & Solid State Chemistry. Encycl. Inorg. Chem.* **1994**, *6*, 3106.

- (4) Kosyakov, V. I.; Vasileva, I. G. *Phosphorus Rings, Clusters, Chains & Layers. Russ. Chem. Rev.* **1979**, *48*, 153.
- (5) Wilkinson, G.; Stone, F. G. A., Eds. *Comprehensive Organometallic Chemistry*; Pergamon: Oxford, UK, 1982.
- (6) Corbridge, D. E. C. *Phosphorus 2000: Chemistry, Biochemistry & Technology*; Elsevier: New York, 2000.
- (7) Tan, K.; Lin, M.-H.; Wu, W.; Zheng, L.-S.; Zhang, Q.-E. *Chem. J. Chin. Univ.* **1999**, *20*, 598.
- (8) Pan, G.-B.; Feng, J.-K.; Ren, A.-M. *Acta Chim. Sin.* **2002**, *60*, 586.
- (9) Pan, G.-B.; Feng, J.-K.; Ren, A.-M. *Chem. J. Chin. Univ.* **2002**, *23*, 893.
- (10) Lu, Y.-P.; Lin, M.-H.; Wang, Y.-G. *Chin. J. Struct. Chem.* **1998**, *17*, 187.
- (11) Liu, C.-Y.; Huang, R.-B.; Zheng, L.-S. *Chem. J. Chin. Univ.* **1997**, *18*, 293.
- (12) Urnežúyius, E.; Brennessel, W. W.; Cramer, C. J.; Ellis, J. E.; Schleyer, P. v. R. *Science* **2002**, *295*, 832.
- (13) Scherer, O. J.; Swarowsky, H.; Wolmershäuser, G.; Kaim, W.; Kohlmann, S. *Angew. Chem., Int. Ed. Engl.* **1987**, *26*, 1153.
- (14) Reddy, A. C.; Jemmls, E. D. *J. Organometallics* **1992**, *11*, 3894.
- (15) Collins, J. B.; Schleyer, P. v. R. *Inorg. Chem.* **1977**, *16*, 152.
- (16) Jemmls, E. D.; Alexandratos, S.; Schleyer, P. v. R.; Streitwieser, A., Jr.; Schaefer, H. F., III *J. Am. Chem. Soc.* **1978**, *100*, 5695.
- (17) Krogh-Jespersen, K.; Chandrasekhar, J.; Schleyer, P. v. R. *J. Org. Chem.* **1980**, *45*, 1608.
- (18) Garrat, P. J. *Aromaticity*; Wiley: New York, 1986.
- (19) Minkin, V. J.; Glukhovesev, M. N.; Simkin, B. Y. *Aromaticity and Antiaromaticity: Electronic and Structural Aspects*; Wiley: New York, 1984.
- (20) Schleyer, P. v. R.; Jiao, H. *Pure Appl. Chem.* **1996**, *68*, 209.
- (21) Krygowski, T. M.; Cvranski, M. K.; Czarnocki, Z.; Hafelinger, G.; Katritzky, A. R. *Tetrahedron* **2000**, *56*, 1783.
- (22) Li, X. W.; Pennington, W. T.; Robinson, G. H. *J. Am. Chem. Soc.* **1995**, *117*, 7578.
- (23) Li, X. W.; Xie, Y.; Schreiner, P. R.; Gripper, K. D.; Crittendon, R. C.; Campana, C. F.; Schaefer, H. F., III; Robinson, G. H. *Organometallics* **1996**, *15*, 3798.
- (24) Xie, Y.; Schreiner, P. R.; Schaefer, H. F., III; Li, X. W.; Robinson, G. H. *J. Am. Chem. Soc.* **1995**, *117*, 7578.
- (25) Robinson, G. H. *Acc. Chem. Res.* **1999**, *32*, 773.
- (26) Li, X.; Kuznetsov, A. E.; Zhang, H. F.; Boldyrev, A. I.; Wang L. S. *Science* **2001**, *291*, 859.
- (27) Kuznetsov, A. E.; Corbett, J. D.; Wang, L. S.; Boldyrev, A. I. *Angew. Chem., Int. Ed.* **2001**, *40*, 3369.
- (28) Kuznetsov, A. E.; Boldyrev, A. I.; Li, X.; Wang, L. S. *J. Am. Chem. Soc.* **2001**, *123*, 8825.
- (29) Fowler, P. W.; Havenith, R. W. A.; Steiner, E. *Chem. Phys. Lett.* **2001**, *342*, 85.
- (30) Fowler, P. W.; Havenith, R. W. A.; Steiner, E. *Chem. Phys. Lett.* **2001**, *359*, 530.
- (31) Kekule, A. *Bull. Soc. Chim. Fr.* **1865**, *3*, 98.
- (32) King, R. B. *Chem. Rev.* **2001**, *101*, 1119.
- (33) Jemmls, E. D.; Schleyer, P. v. R. *J. Am. Chem. Soc.* **1982**, *104*, 4781.
- (34) Katritzky, A. R.; Barczynski, P.; Musumarra, G.; Pisano, D.; Szafran, M. *J. Am. Chem. Soc.* **1989**, *111*, 7.
- (35) Jug, K.; Koster, A. M. *J. Phys. Org. Chem.* **1991**, *4*, 163.
- (36) Schleyer, P. v. R.; Freeman, P. K.; Jiao, H.; Goldfuss, B. *Angew. Chem., Int. Ed. Engl.* **1995**, *34*, 337.
- (37) Bird, C. W. *Tetrahedron* **1996**, *52*, 9945.
- (38) Schleyer, P. v. R.; Maerker, C.; Dransfeld, A.; Jiao, H.; Homm, N. v. E. *J. Am. Chem. Soc.* **1996**, *118*, 6317.
- (39) Schleyer, P. v. R.; Jiao, H. *Pure Appl. Chem.* **1996**, *68*, 209.
- (40) Goldfuss, B.; Schleyer, P. v. R.; Hampel, F. *Organometallics* **1996**, *15*, 1998.
- (41) Becke, A. D. *J. Chem. Phys.* **1993**, *98*, 5648.
- (42) Mclean, A. D.; Chandler, G. S. *J. Chem. Phys.* **1980**, *72*, 5639.
- (43) Clark, T.; Chandrasekhar, J.; Spitznagel, G. W.; Schleyer, P. v. R. *J. Comput. Chem.* **1983**, *98*, 5648.
- (44) Frisch, M. J.; Pople, J. A.; Binkley, J. S. *J. Chem. Phys.* **1984**, *80*, 3265.
- (45) Parr, R. G.; Yang, W. *Density-Functional Theory of Atoms and Molecules*; Oxford University Press: Oxford, U.K., 1989.
- (46) Möller, C.; Plesset, M. S. *Phys. Rev.* **1934**, *46*, 618.
- (47) Carpenter, J. E.; Weinhold, E. *J. Mol. Struct.: THEOCHEM* **1988**, *169*, 41.
- (48) Reed, A. E.; Curtiss, L. A.; Weinhold, F. *Chem. Rev.* **1988**, *88*, 899.
- (49) Reed, A. E.; Weinstock, R. B.; Weinhold, F. *J. Chem. Phys.* **1985**, *88*, 735.
- (50) Frisch, M. J.; Trucks, G. W.; Schlegel, H. B.; Scuseria, G. E.; Robb, M. A.; Cheeseman, J. R.; Zakrzewski, V. G.; Montgomery, J. A., Jr.; Stratmann, R. E.; Burant, J. C.; Dapprich, S.; Millam, J. M.; Daniels, A.

D.; Kudin, K. N.; Strain, M. C.; Farkas, O.; Tomasi, J.; Barone, V.; Cossi, M.; Cammi, R.; Mennucci, B.; Pomelli, C.; Adamo, C.; Clifford, S.; Ochterski, J.; Petersson, G. A.; Ayala, P. Y.; Cui, Q.; Morokuma, K.; Malick, D. K.; Rabuck, A. D.; Raghavachari, K.; Foresman, J. B.; Cioslowski, J.; Ortiz, J. V.; Baboul, A. G.; Stefanov, B. B.; Liu, G.; Liashenko, A.; Piskorz, P.; Komaromi, I.; Gomperts, R.; Martin, R. L.; Fox, D. J.; Keith, T.; Al-Laham, M. A.; Peng, C. Y.; Nanayakkara, A.; Challacombe, M.; Gill, P.

M. W.; Johnson, B.; Chen, W.; Wong, M. W.; Andres, J. L.; Gonzalez, C.; Head-Gordon, M.; Replogle, E. S.; Pople, J. A. *Gaussian 98*, Revision A.9; Gaussian, Inc.: Pittsburgh, PA, 1998.

(51) Schaftenaar, G. *MOLDEN 3.7*; CAOS/CAMM Center, The Netherlands. 1998.

(52) Corbridge, D. E. C. *Top. Phosphorus Chem.* **1966**, 3, 57.